Self-assembly, Cytocompatibility, and Interactions of Desmopressin with Sodium Polystyrene Sulfonate

Ana B. Caliari[1], Renata N. Bicev[1,2], Caroline C. da Silva[1], Sinval E. G. de Souza[1], Marta G. da Silva[1], Louise E. A. Souza[1], Lucas R. de Mello[1,3], Ian W. Hamley[3], Guacyara Motta[4], Jéril Degrouard[2], Guillaume Tresset[2], Alexandre J. C. Quaresma[1], Clovis R. Nakaie[1], and Emerson R. da Silva[1,*]

[1] Departamento de Biofísica, Universidade Federal de São Paulo, São Paulo 04062-000, Brazil

[2] Université Paris-Saclay, CNRS, Laboratoire de Physique des Solides, 91405 Orsay, France

[3]Department of Chemistry, University of Reading, Reading RG6 6AD, United Kingdom

[4]Departamento de Bioquímica, Universidade Federal de São Paulo, São Paulo 04044-020, Brazil

Supplementary methods:

Preparation of model membranes: The interactions between desmopressin and lipids were investigated using model membranes prepared from a mixture of phosphatidylcholine, oleic acid, and myristic acid in a 7:2:1 mass ratio. This formulation roughly reproduces the lipid fraction found in biomembranes, which are mostly composed of phospholipids, with phosphatidylcholine being the most abundant.[1] Additionally, fatty acids, among which oleic acid is a major representative, and myristic acid, present at lower concentrations, are also components of these membranes.[2,3] L-α-phosphatidylcholine from soy bean was purchased from Avanti Polar (product code # 441601, M_w = 775 g·mol^{-1}), while oleic acid (#O1008, M_w = 282.5) and myristic acid (#70079, M_w = 228.4) were acquired from Sigma-Aldrich and used as received. The lipids were weighted at the appropriate masses and solubilized in chloroform. The mixture was vigorously stirred until complete homogenization was achieved. Subsequently, the content (approximately 10 ml) was transferred to a round-bottom glass flask, and a stream of dry nitrogen was introduced into the flask and maintained for about 4 hours until complete evaporation of the solvent occurred, resulting in the formation of a lipid film with an average molecular mass calculated at M_w = 622.5 g·mol^{-1}. This lipid film was reconstituted in PBS buffer (10 mM, pH = 7.2) to form a stock solution of vesicles at a concentration of 40 mg·mL^{-1} (0.64 mM). Samples for cryo-TEM and quenching assays were prepared by diluting these stocks to final concentrations of 1 mg·mL^{-1}. These model membranes have proven useful in previous analysis of peptide-membrane interactions by our group.[4]

High Performance Liquid Chromatography and mass spectroscopy data:
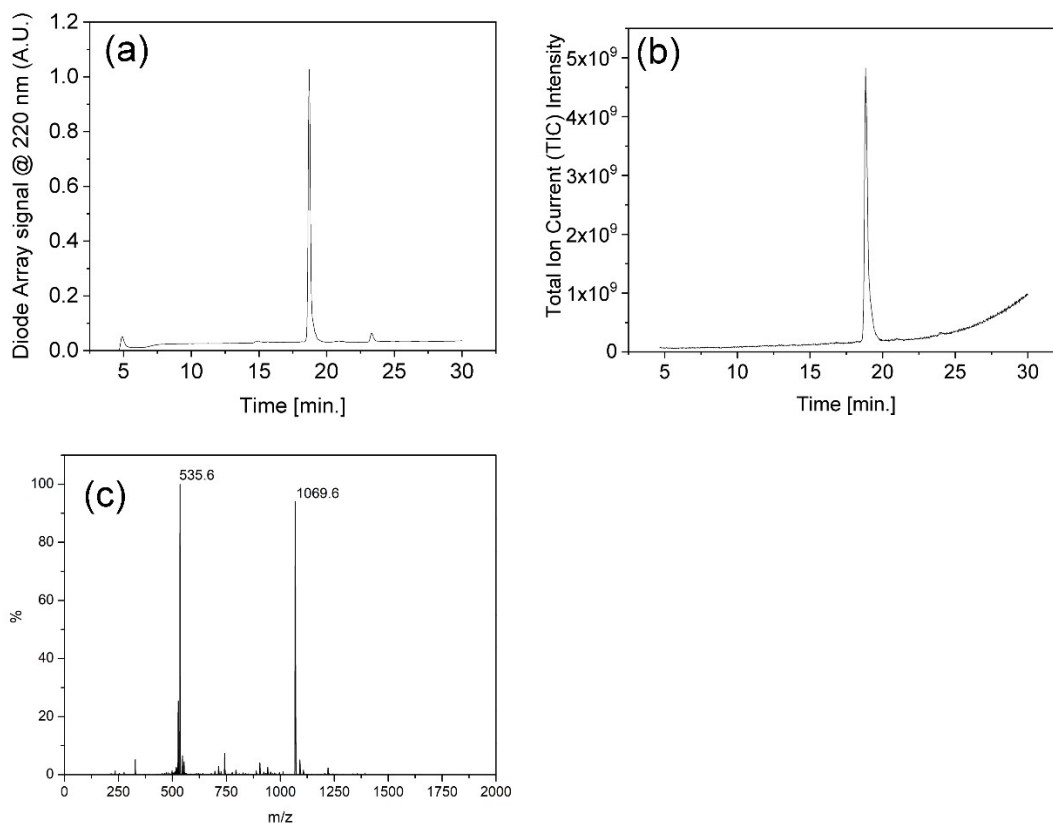
Figure S1: HPLC data showing the diode array channel absorbance at 220 nm (a) and the total ion current intensity (b). Desmopressin elution time is found at 18.8 min. In (c), the mass spectrum exhibits fragments found in the corresponding eluted fraction.

SAXS models used for data fitting:

SAXS data have been fitted using models available in the library of the SASFit package.[5] We reproduce below the relevant equations from the models available in the SASFit manual to provide the reader with an overview of the parameters obtained from the fitting. Further mathematical details on the models used in our analyses can be found in the manual of SASFit (https://sasfit.org/) or in comprehensive texts on SAXS data treatment.[6–9] Data from desmopressin solutions were fitted using a combination of a power law plus a generalized Gaussian chains form factor:

$$I(q) \cong Bkg + \frac{A}{q^{\alpha}} + \frac{I_0 \cdot U^{\frac{1}{2v}} \cdot \Gamma\left(\frac{1}{2v}\right) - \Gamma\left(\frac{1}{v}\right) - U^{\frac{1}{2v}} \cdot \Gamma\left(\frac{1}{2v}, U\right) + \Gamma\left(\frac{1}{v}, U\right)}{v \cdot U^{\frac{1}{v}}} \qquad (S1)$$

Where U is given by:

$$U = (2v + 1)(2v + 2)\frac{q^2 \cdot R_g^{\,2}}{6} \qquad (S2)$$

In equation (S1), *Bkg* is an additive constant accounting for a flat background. The second term is a power law that describes the linear decay (in log-log representation) observed at the low-q region, where A is a factor weighing the contribution of the power law component to the whole scattering. In our analyses, the scattering at the low-q region is ascribed to large desmopressin aggregates whose dimensions are larger than the experimental window achievable in our experiments (see main text). The parameter α is the scaling exponent, which carries structural information on the fractal dimensionality of aggregates and, depending on the value it assumes, two types of fractal aggregates can be identified:[7,10] if $2 < \alpha < 3$, it indicates that the sample is populated by mass fractals and their fractal dimension is given by $D_m = \alpha$. If $3 < \alpha < 4$, it indicates presence of surface fractals, and the fractal dimension is given by $D_s = 6 - \alpha$. The third term is more complex, and it corresponds to the generalized Gaussian chain form factor.[6] In our case here, this term is introduced in the model to describe scattering at higher q-values which is ascribed to the presence of free peptide chains in the solutions. The symbol Γ represents the gamma function, and the parameters v and R_g are associated with the Flory exponent and the gyration radius of the chains, respectively. The Flory exponent carries information on the interaction between peptide chains and the surrounding solvent: a $v = 0.6$ indicates that the chain is swollen (good solvent), a $v = 0.33$ points to a collapsed coil (poor solvent), and a $v = 0.5$ suggests a theta solvent (meaning that the chains interact equally with the solvent and themselves).[11] The gyration radius, Rg, is a measure of the size of the region occupied by the chain and is analogous to the radius of an equivalent sphere that would occupy the same volume as the chains.

In the case of NaPSS solutions, SAXS data were fitted by using a Porod cylinder form factor whose expression is given by:

$$P_{cyl}(q,R,L) = \frac{2}{qL}(\Delta\eta R^2 L)^2 \times \left\{ Si_{\frac{\pi}{2}}(qL)\Lambda_1^2(qR) - \frac{2\Lambda_2(2qR) - \Phi(2qR)}{qL} - \frac{\sin(qL)}{(qL)^2} \right\} \quad (S4)$$

Where the modified sine integral function is given by:

$$Si_{\frac{\pi}{2}}(qL) = \left(Si(qL) + \frac{\cos(qL)}{qL} + \frac{\sin(qL)}{(qL)^2} \right) \xrightarrow{qL\to\infty} \frac{\pi}{2} \quad (S5)$$

And $\Lambda_1(x) = \frac{2}{qL}J_1(qL)$, $\Lambda_2(x) = \frac{8}{(qL)^2}J_2(qL)$, and $\Phi(x) = \frac{2}{(qL)^2}[1 - \Lambda_1(qL)]$.

With J_1 and J_2 denoting first kind Bessel functions of 1st and 2nd order, respectively. R is the radius of the cylinder, L is the length (in our case arbitrarily assumed to be long and fixed at 1000 nm), and $\Delta\eta$ is the difference between electron densities of the scattering objects (peptide, polymer, complexes, etc.) and the surrounding solvent.

Cryo-TEM image of lipid vesicles used in quenching assays:
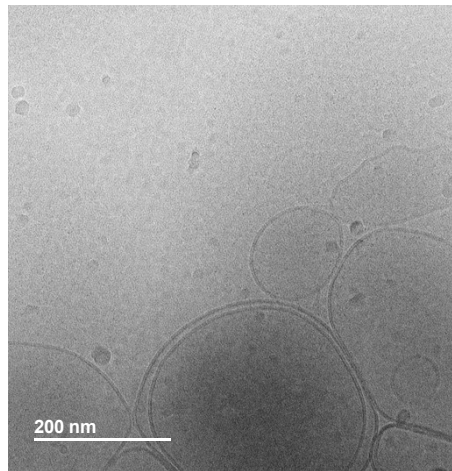
Figure S2: Cryo-TEM image of lipid vesicles used in quenching assays to investigate interactions with desmopressin.

Study of yield during the cleavage step:

Table S1. Summary of parameters showing the yield during the cleavage step.

Dilution (mmol:litre)	Peak area			Yield	
	Standard	Sample	%	mg	%

1:1	1.889.981	3.161.251	95	167.3	17
1:3	1.896.784	2.123.855	90	335.9	34
1:6	1.889.981	1.023.936	89	325.0	33
1:9	1.889.981	772.776	92	368.0	38

Obs: Cleavage with 1 mmol of peptide resin, extraction with ethyl acetate, and injection volume of 10 μL.
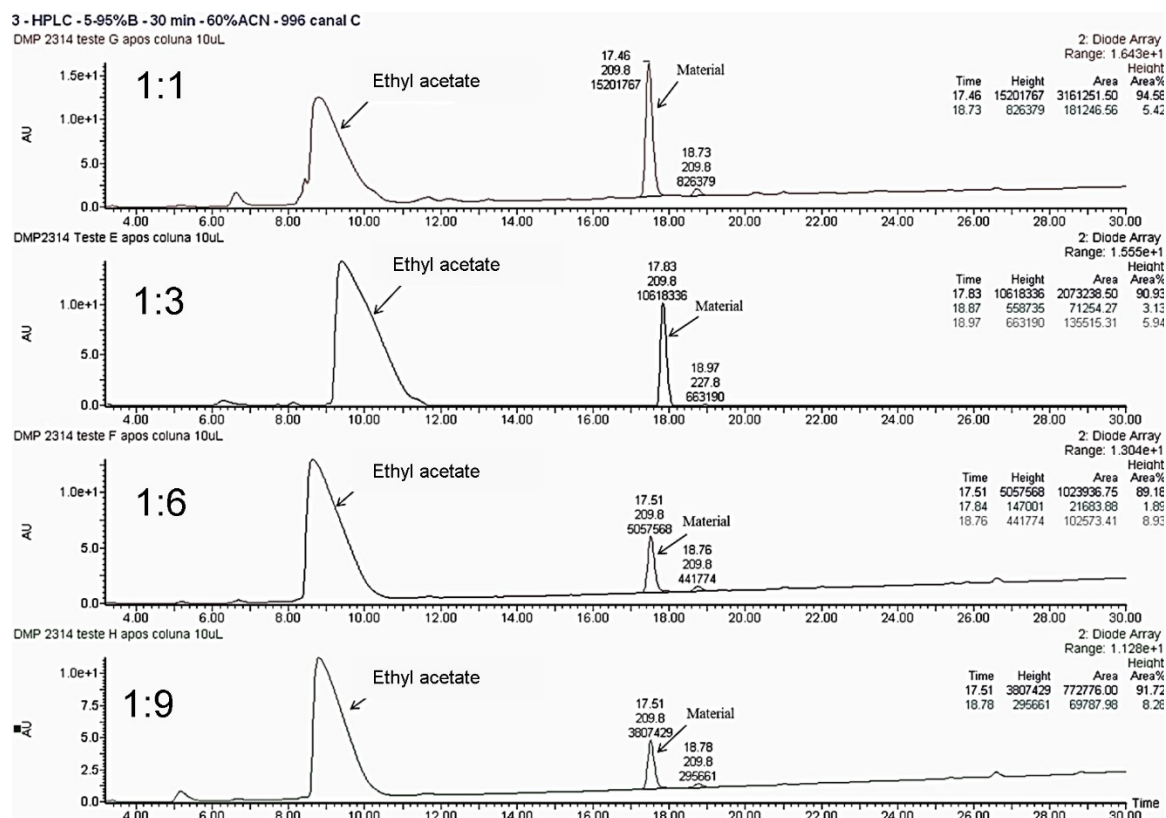
Figure S3. Chromatography profiles of samples at the different dilutions.

ThT fluorescence in the presence of lipid membranes:
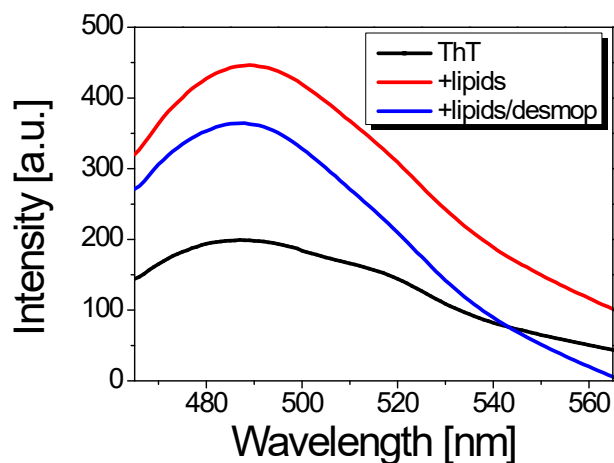
Figure S4. ThT fluorescence in mixtures containing 1 mg/mL lipids or 1 mg/mL lipids and 0.5 mg/mL desmopressin.

Supplementary CD experiments in protamine/NaPSS:
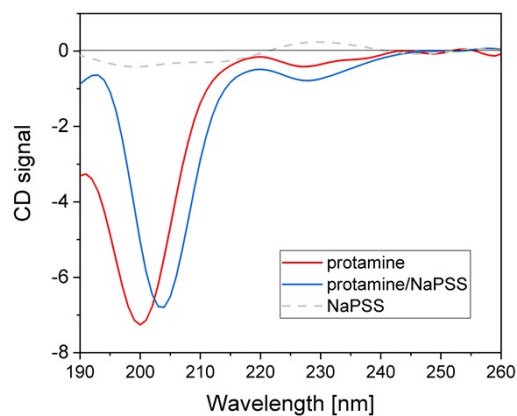
Figure S5. CD spectra of solutions containing mixtures of 128 μg·mL^{-1} NaPSS with 100 μg·mL^{-1} protamine, a peptide which does not exhibit aggregating capabilities.

Supplementary AFM images:
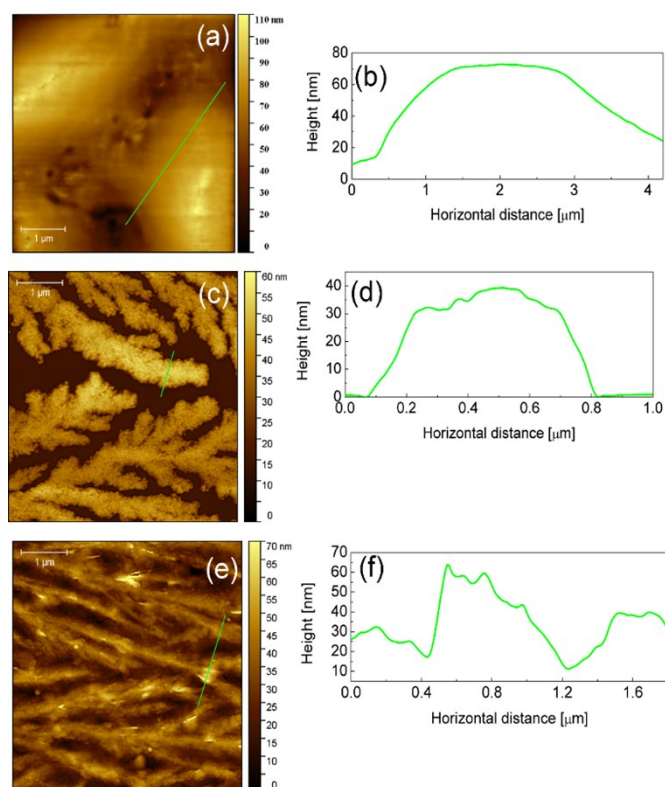
Figure S6. Height profiles across images shown in the main text (Figures 5, 6, and 7). (a) and (b) desmopressin; (c) and (d) NaPSS; (e) and (f) desmopressin/NaPSS.
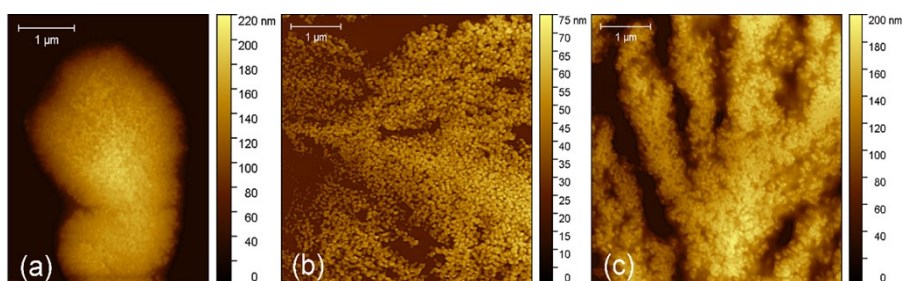
Figure S7. Topography images of NaPSS on gold substrates. (a) polymer aggregate; (b) spread NaPSS grains; (c) polymer ramifications.

Average infrared spectra shown in Figures 5 and 6:
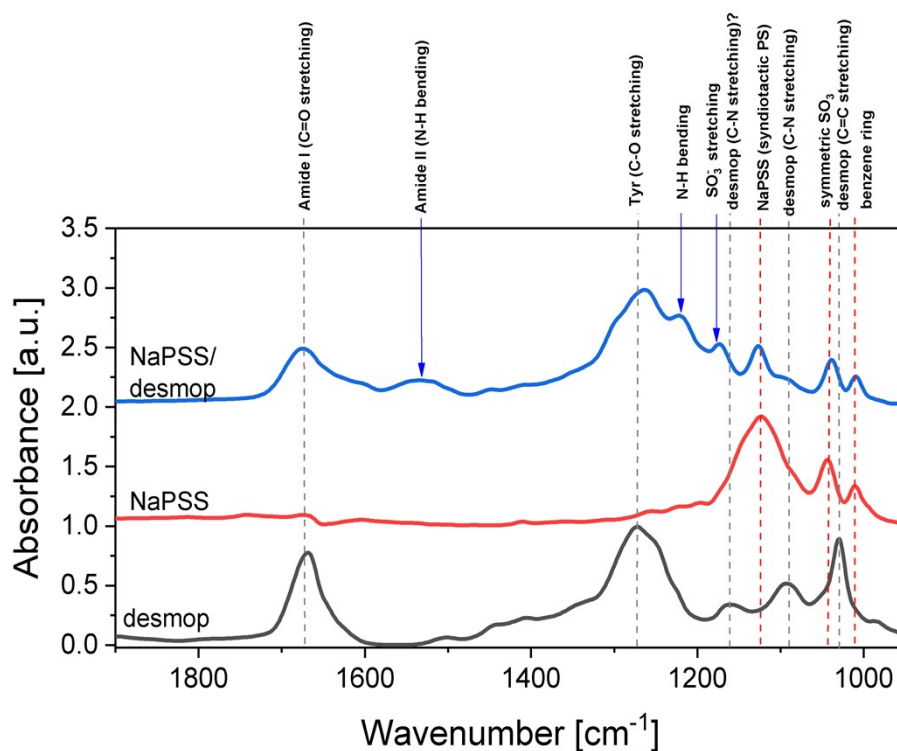
Figure S8. Average spectra from infrared are shown in Figures 5b, 5d, and 6b (main text). Dashed lines indicate resonances associated with desmopressin (gray) and NaPSS (red). Blue arrows highlight new peaks that emerge in the spectra of NaPSS/desmopressin complexes with their tentative assignments.

Resazurin assays data:

Table S2. Data of cell viability obtained in resazurin assays. The raw data (in black) represent the fluorescence of resorufin, which results from the reduction of resazurin in the mitochondria of viable cells. Percentages (in blue) were determined relative to the average of all control well on each plate. Total averages (red) were determined from viability percentages obtained on both days. Significance was assessed using the Welch's t-test (unequally variances).

MCF7 — 1st trial

		DMP				PSS					DMP/PSS			
		CTRL	1000	500	250	CTRL	1000	500	250		CTRL	1000	500	250
		34866	33007	35532	33922	37999	32753	34549	33221		35965	32999	34945	34221
Avg CTRL day 1	36154.1	37529	34486	36852	33533	38173	32170	35671	33744		33873	32541	33131	33744
		36501	32825	34769	37947	37336	32680	33468	34503		33145	32961	33802	34830
		96.4	91.3	98.3	93.8	105.1	90.6	95.6	91.9		99.5	91.3	96.7	94.7
% of control day 1		103.8	95.4	101.9	92.8	105.6	89.0	98.7	93.3		93.7	90.0	91.6	93.3
		101.0	90.8	96.2	105.0	103.3	90.4	92.6	95.4		91.7	91.2	93.5	96.3

MCF7 — 2nd trial

		DMP				PSS					DMP/PSS			
		CTRL	1000	500	250	CTRL	1000	500	250		CTRL	1000	500	250
		24835	24594	23032	26759	25361	22296	21545	20730		25237	22865	19806	21703
Avg CTRL day 2	23035.9	19586	25001	22257	22914	22442	25695	22466	20546		23472	22068	18996	23369
		23896	24380	22939	20767	23427	25831	22837	24984		19067	22063	19621	27967
		107.8	106.8	100.0	116.2	110.1	96.8	93.5	90.0		109.6	99.3	86.0	94.2
% of control day 2		85.0	108.5	96.6	99.5	97.4	111.5	97.5	89.2		101.9	95.8	82.5	101.4
		103.7	105.8	99.6	90.2	101.7	112.1	99.1	108.5		82.8	95.8	85.2	121.4
Combined AVG	100.0		99.8	98.8	99.6		98.4	96.2	94.7			93.9	89.2	100.2
Combined STD	7.7		8.2	2.2	9.7		10.7	2.7	7.1			3.6	5.5	10.8

MDA-231 — 1st trial

		DMP				PSS					DMP/PSS			
		CTRL	1000	500	250	CTRL	1000	500	250		CTRL	1000	500	250
		32240	29183	31378	31162	31669	19198	24996	26538		36824	20159	24940	27991
Avg CTRL day 1	32096.0	32532	32578	31953	32750	30677	22532	23962	27965		30100	22524	26210	26363
		32539	30037	32745	32308	30944	23443	24688	28517		31339	20404	26149	27895
		100.4	90.9	97.8	97.1	98.7	59.8	77.9	82.7	0.0	114.7	62.8	77.7	87.2
		101.4	101.5	99.6	102.0	95.6	70.2	74.7	87.1	0.0	93.8	70.2	81.7	82.1
		101.4	93.6	102.0	100.7	96.4	73.0	76.9	88.8	0.0	97.6	63.6	81.5	86.9

MDA-231 — 2nd trial

		DMP				PSS					DMP/PSS			
		CTRL	1000	500	250	CTRL	1000	500	250		CTRL	1000	500	250
		18985	19344	19249	19740	20778	13242	13756	15966		21106	14075	15838	16904
Avg CTRL day 2	19539.7	18379	19634	19603	20120	19722	13430	14094	16120		19937	14221	15934	17119
		19244	19338	20035	21595	18775	13558	13965	16820		18931	14459	15345	18572
		97.2	99.0	98.5	101.0	106.3	67.8	70.4	81.7		108.0	72.0	81.1	86.5
		94.1	100.5	100.3	103.0	100.9	68.7	72.1	82.5		102.0	72.8	81.5	87.6
		98.5	99.0	102.5	110.5	96.1	69.4	71.5	86.1		96.9	74.0	78.5	95.0
Combined AVG	100		97.4	100.1	102.4		68.2	73.9	84.8			69.2	80.3	87.6
Combined STD	5.3		4.2	1.9	4.5		4.5	3.1	2.9			4.8	1.7	4.2

Supplementary references

1   G. L. Nicolson, *Biochim. Biophys. Acta-Biomembranes*, 2014, **1838**, 1451–1466.

2   J. Schumann, A. Leichtle, J. Thiery and H. Fuhrmann, *PLoS One*, 2011, **6**, 1–8.

3   V. S. Shramko, Y. V Polonskaya, E. V Kashtanova, E. M. Stakhneva and Y. I. Ragino, *Biomolecules*, 2020, 10.

4   M. M. L. Ferreira, S. E. G. de Souza, C. C. da Silva, L. E. A. Souza, R. N. Bicev, E. R. da Silva and C. R. Nakaie, *Biochemistry*, 2023, **62**, 2530–2540.

5   I. Bressler, J. Kohlbrecher and A. F. Thunemann, *J. Appl. Crystallogr.*, 2015, **48**, 1587–1598.

6   J. S. Pedersen, *Adv. Colloid Interface Sci.*, 1997, **70**, 171–210.

7   J. Teixeira, *J. Appl. Crystallogr.*, 1988, **21**, 781–785.

8   I. W. Hamley, *Small-Angle Scattering: Theory, Instrumentation, Data and Applications*, Wiley, Chichester, 1st edn., 2021.

9   T. Zemb and P. Lindner, *Neutrons, X-rays and light : scattering methods applied to soft condensed matter*, Elsevier, Amsterdam ; Boston, 1st edn., 2002.

10   B. Hammouda, *J. Chem. Phys.*, 2010, **133**, 84901.

11   I. W. Hamley, in *Introduction to Soft Matter*, John Wiley & Sons, Ltd, 2007, pp. 39–110.